# Biofilm Formation during Hexadecane Degradation and the Effects of Flow Field and Shear Stresses

Christer Fjeld[1,2] and Reidar Barfod Schüller[1]

*[1]Dept. of Chemistry, Biotechnology and Food Science, Norwegian University of Life Sciences, P.O.Box 5003, N-1432 Ås, Norway .[2]FRAS Technology AS, Kongeveien 30. 1430 Ås, Norway*

ABSTRACT

In this study, we developed a model of the flow field and the shear forces which the biofilm experiences in the CDC biofilm reactor, using Comsol Multiphysics software. The biofilms were formed on stainless steel (316L) coupons and cultured using mineral salt media and hexadecane (10% w/v) as the sole source of carbon and energy for growth. Our model shows that the biofilms formed on the side facing toward the glass wall are experiencing close to zero shear stress with some oscillations. The biofilms that are formed towards the baffled stirrer bar are experiencing higher shear stresses in the range of 0.35-0.39 Pa. The model is based on a stirring rate of 170 rpm and a fluid viscosity of 2 mPas at a shear rate of 20 $s^{-1}$. The dispersion of the 10% hexadecane/ mineral media mixture was unstable and depended on shear rate. This causes the dispersed hexadecane droplets to separate from the water phase at low mixer speeds. Using confocal laser scanning microscopy to visualize biofilm architecture, we found that the flow field and shear stresses in the CDC biofilm reactor, has a profound impact on the biofilms formed on stainless steel (316L) during hexadecane degradation. The biofilms formed when exposed to 0.35-0.39 Pa were homogenous and had a thickness of approximately 25µm, thus the shear stress will slough off any cells exceeding this level of shear stress. On the other hand, biofilms formed when exposed to close to zero shear stress, were heterogeneous, showing "valleys and peaks". This level of shear stress is negligible, and the biofilms grew unaffected of shear stress to a maximum thickness of approximately 35µm.

## INTRODUCTION

Biofilm are multi cellular structures formed by most microorganisms, which are significantly different from their planktonic counterparts[1]. Biofilms are formed on surfaces and interfaces, and are characterized by microbial cells embedded in a self generated hydrated matrix[2, 3]. Biofilm structure and biovolume are affected by several factors, such as microbial diversity[4]. In addition, flow dynamics and the shear stress, opposing surfaces have previously been shown to have a strong impact on structure, diversity, and biovolume of the biofilms[5-7]. Therefore, biofilms can be considered as a material with viscoelastic properties[8].

In this study we set out explore and quantify the flow field and shear stresses that biofilms experiences in the CDC biofilm reactor and how this affects biofilm structure during hexadecane degradation. The flow field and shear stresses in the CDC biofilm reactor was modelled using Comsol Multiphysics. To visualize biofilm we used confocal laser scanning microscopy.

## MATERIALS AND METHODS

### Bacteria used in the study

In this study we used the hydrocarbon degrading bacterium, *Acinetobacter* sp dsm 17874[9]. Acinetobacters are ubiquitous in nature, Gram negative, strict aerobic and coccobacilli shaped bacteria that belongs to the Gammaproteobacteria.

### Growing biofilms

Mono species Biofilms formed by *Acinetobacter* sp dsm 17874 were grown in the CDC biofilm reactor, Figure 1, supplied with coupons of stainless steel (316L). The CDC biofilm reactor was supplied with 250ml minimal salt media (2.5g $Na_2HPO_4$ x $2H_2O$, 1.3g $KH_2PO_4$, 0.2g $MgSO_4$ x $7H_2O$, 1ml Hoagland's solution, 0.5ml 1% $FeSO_4$, 0.5ml 1% $Na_2MoO_4$ $L^{-1}$) and 25ml Hexadecane as the sole source of carbon and energy for growth. The biofilms were grown at 25°C. The coupons were removed from the biofilm reactor after 48 hours.

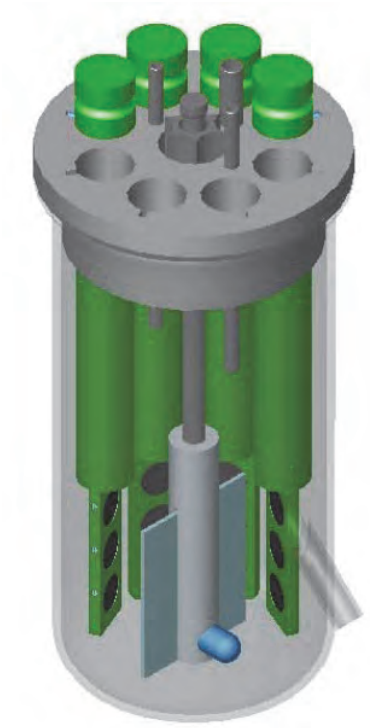

Figure 1. CDC biofilm reactor.

### Modeling flow field and shear stress in the CDC biofilm reactor

Before we could model the flow field and shear stresses in the CDC biofilm reactor we determined the fluid viscosity of the hexadecane water mixture. Viscosity of the 10% hexadecane mineral media mixture was measured in a MCR301 rheometer (Anton Paar) using a ST24-2D/2V/2V-30/129 mixer in a CC27 cup. To estimate the rotational velocity of the baffled stir bar in the CDC biofilm reactor, we used a camera with 30 frames $s^{-1}$. With these parameters, in addition to measuring relevant distances in the CDC biofilm reactor, we could use Comsol Multiphysics version 3a software to model the different flow regimes and shear forces that the biofilms will experience in such device. Both a 3D, Figure 2, and a 2D axisymmetric model were built.

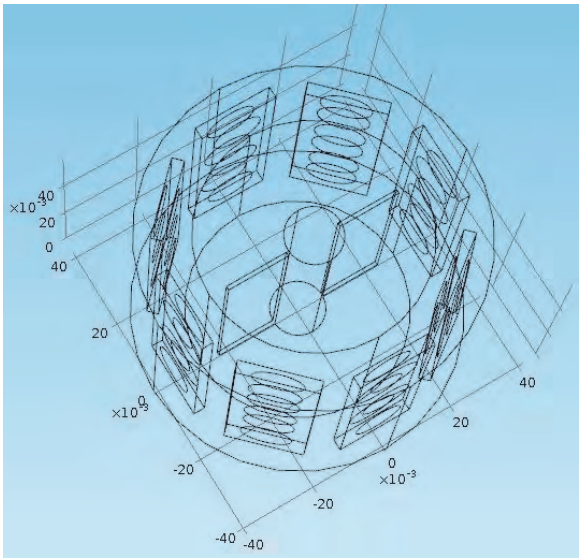


Figure 2. 3D model of the lower fluid filled part of the biofilm reactor.

The rotating flow was modelled using "Rotating Machinery, Turbulent Flow, k-ε *(rmspf)*. The physical model was "Compressible flow (Ma<0.3)", and the turbulence model was "RANS, k-ε".

The meshing was set to "Physics-controlled mesh", and the element size was set to "Coarse". The resulting mesh size was 571208 elements for the 3D model.

Solving the 3D model for a 10 s time interval required approximately 100 hours calculation time. The 2D model found a solution for the same time interval in approximately 3 hours.

Fluorescent hybridization in situ hybridization (FISH)

The optimal probe and formamide concentration used in FISH, was determined on a planktonic culture of Acinetobacter sp dsm 17874 according to Malic *et al*[10] using the Acinetobacter specific probe, ACA (Cy3 - 5`ATCCTCTCCCATACTCTA 3`)[11]. However, the probe was of DNA chemistry and not PNA chemistry. The optimal formamide and probe concentration used in this study was found to be 20% w/v and 10µg $ml^{-1}$ respectively. Before FISH was undertaken on the biofilms, the coupons were gently submerged in sterile water three times to remove most of the hexadecane film on top of the biofilm. FISH procedure on the biofilms was performed as described in[12] using the ACA probe. However, the following modifications were made; the coupons was placed in 10ml glass test tubes and instead of one wash of 50ml, the washing was executed two times using 5ml of wash buffer. After the FISH procedure, the biofilms was counter stained with 2.0 ml Nile red solution (10µg $ml^{-1}$ in 50% PBS/ glycerol, made from stock solution 1mg ml-1 Nile Red in acetone) to visualize hydrocarbon droplets, during 30 minutes at 37$^{o}$C. After incubation, the biofilms was placed in 5ml of 0.91% NaCl. Finally, prior to confocal laser scanning microscopy analysis, biofilm samples were imbedded in 5µl mowiol 4- 88 (Poly sciences) as recommended by the manufacturer. A cover glass was put on top the embedded biofilm coupons and stored overnight at room temperature.

Confocal laser scanning microscopy (CLSM)

The CLSM investigation was undertaken, using a Carl Zeiss LSM 710 confocal microscope supplied with the ZEN software. The microscope was fitted with Plan-Apochromat 63/1.4 oil immersion objective. To detect signals from the Cy3 fluorophore, the 550nm laser line was used. Nile red was excited using the helium neon laser with wavelength of 443nm.

RESULTS

Flow field and shear stresses in the CDC biofilm reactor

The dynamic viscosity of water containing 10% hexadecane was 2 mPas at a shear rate of 20 $s^{-1}$ (Figure 3). The dispersion of hexadecane droplets in the water phase was unstable and separated rapidly when the stirring stopped. The viscosity of the hexadecane/ water mixture was clearly a function of the mixing intensity (the stirring speed or shear rate), which resulted in separation of the dispersed droplet from the water when the shear rate was reduced.

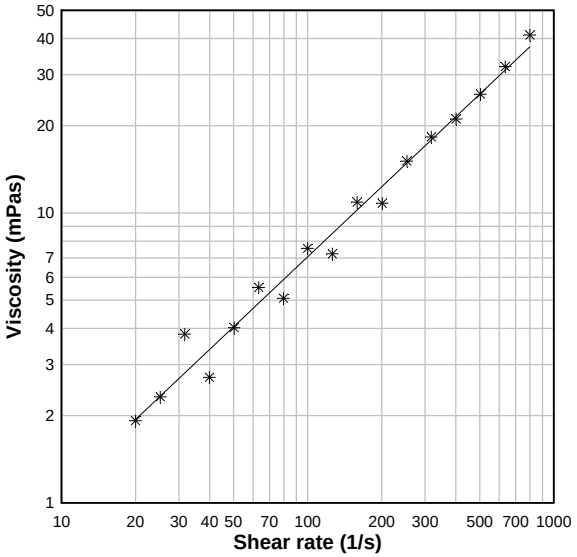


Figure 3. Viscosity versus shear rate for water added with 10% hexadecane at 25 °C.

The flow field in the CDC biofilm reactor was equal for all the twenty four coupons in the reactor, based on a 3D model of the reactor, constructed in Comsol Multiphysics (data not shown). The model shows that the flow field reached steady state after approximately three seconds. Diagrams showing the steady state flow field and the shear rate distribution are shown in Figure 4**Error! Reference source not found.** and Figure 5, respectively. However, some oscillations in the shear stress occurred due to the rotating baffled stir bar (Figure 6).

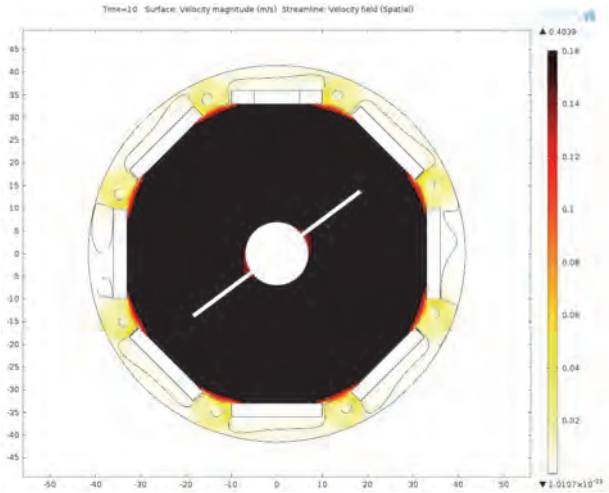

Figure 4. 2D steady state velocity field.

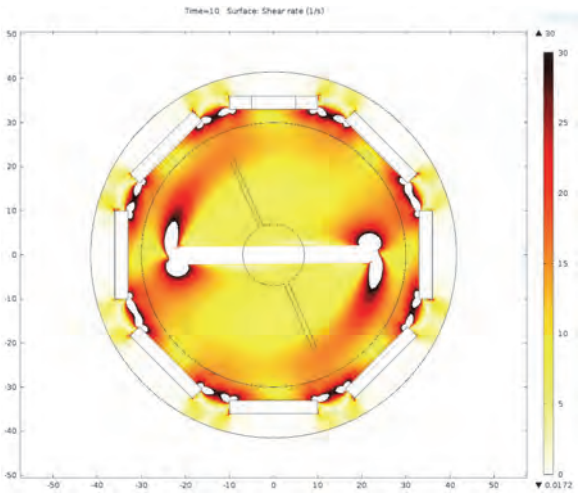

Figure 5. 2D shear rate distribution.

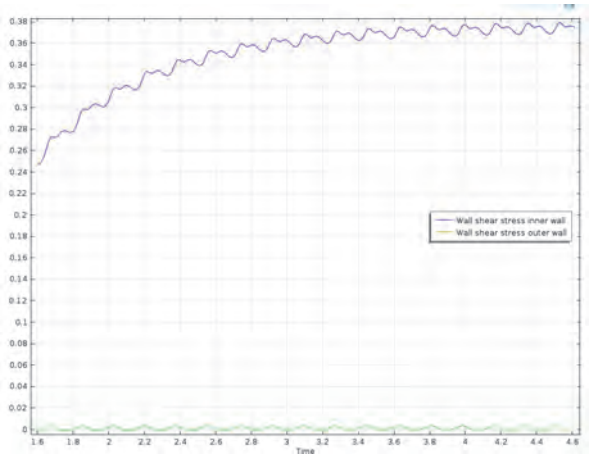


Figure 6. Resulting shear stress (Pa) on coupons. The lower graph shows the shear stress on the side facing towards the glass wall. The upper graph shows the shear stress on the side facing towards the baffled stir bar. Time at the x axis is in seconds.

## Biofilm structure and the role of shear stress

The shear forces which the biofilms experience in the CDC biofilm reactor have a significant impact on biofilm structure. Figure 7 and Figure 8 show the biofilms formed during very low (close to zero) shear force and shear force in the range of 0.36 - 0.39 Pa, respectively. The results from the 3D model showed that the wall shear stress on the coupons was independent of vertical position in the biofilm reactor.

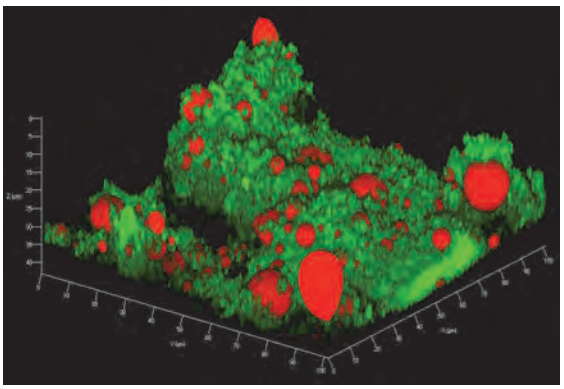

Figure 7. Biofilm formed when exposed to very low shear stress. Green indicates bacteria and red indicates hexadecane droplets.

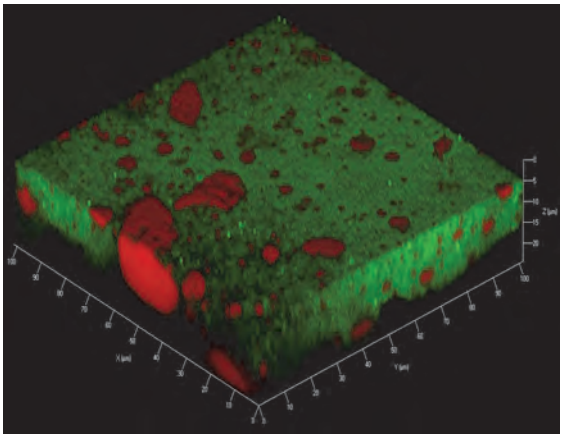

Figure 8. Biofilm formed when exposed to shear stress in the range of 0.36 – 0.39 Pa. Green indicates bacteria and red indicates hexadecane droplets.

## DISCUSSION

The CDC biofilm reactor is common device in the study of biofilms. To our knowledge, this is the first time the effect of the flow field and shear stresses in the CDC biofilm reactor, which the biofilms are experiencing during hydrocarbon degradation, has been investigated. Comsol Multiphysics has previously been shown to be a reliable tool in modelling flow field and shear forces[13, 14]. With emphasis on this previous studies, we can rely on the model we have made, assessing the flow field and shear forces in CDC biofilm reactor. The model also predicts that the flow field and shear forces are equal for all coupons in the CDC biofilm reactor. However, we have not modelled the dissolved oxygen distribution in the CDC biofilm reactor. Microbial oxygen consumption could result in different availability for oxygen in the CDC biofilm reactor. Thus oxygen availability is important in biofilm formation[15]. The use of hexadecane as the sole source of carbon and energy for growth used in this study could eliminate this possible bias, due to the higher oxygen solubility and diffusion rate in hexadecane than in water[16]. Consequently, hexadecane has been shown beneficial in enhancing oxygen transfer, ensuring homogenous distribution of oxygen throughout the fluid filled compartment of the reactor[17]. The viscosity of the fluid is important in the resulting shear stress on the coupons. The 10% hexadecane/ water mixture had a dynamic viscosity of 2 mPas at a shear rate of 20 $s^{-1}$.The mixture was unstable and the viscosity was dependent on the shear rate. This results in the separation of the dispersed hexadecane droplets from the water phase, when the shear rate is reduced.

The flow field and shear stress in the CDC biofilm reactor was close to zero on the side of the coupons that faces towards the glass wall. The resulting biofilm showed structural heterogeneity, which grew unaffected of shear stress. The biofilm formed during higher shear stress was flat due to the increasing shear stress as the distance from the surface of the coupon increases. This causes the cells growing above the flat surface to be sloughed from the biofilm surface.

## REFERENCES

1. Hall-Stoodley, L., J.W. Costerton, and P. Stoodley, (2004), "Bacterial biofilms: from the Natural environment to infectious diseases", *Nat Rev Micro*, **2**(2): p. 95-108.

2. Sutherland, I.W., (2001), "The biofilm matrix - an immobilized but dynamic microbial environment", *Trends in Microbiology*, **9**(5): p. 222-227.

3. Costerton, J.W., Z. Lewandowski, D.E. Caldwell, D.R. Korber, and H.M. Lappin-Scott, (1995), "Microbial biofilms", *Annu. Rev. Microbiol.*, **49**: p. 711-745.

4. Burmølle, M., J.S. Webb, D. Rao, L.H. Hansen, S.J. Sorensen, and S. Kjelleberg, (2006), "Enhanced Biofilm Formation and Increased Resistance to Antimicrobial Agents and Bacterial Invasion Are Caused by Synergistic Interactions in Multispecies

Biofilms", *Appl. Environ. Microbiol.*, **72**(6): p. 3916-3923.

5. Rochex, A., J.-J. Godon, N. Bernet, and R. Escudié, (2008), "Role of shear stress on composition, diversity and dynamics of biofilm bacterial communities", *Water Research*, **42**(20): p. 4915-4922.

6. Stoodley, P., Z. Lewandowski, J.D. Boyle, and H.M. Lappin-Scott, (1999), "Structural deformation of bacterial biofilms caused by short-term fluctuations in fluid shear: An in situ investigation of biofilm rheology", *Biotechnology and Bioengineering*, **65**(1): p. 83-92.

7. Pereira, M.O., M. Kuehn, S. Wuertz, T. Neu, and L.F. Melo, (2002), "Effect of flow regime on the architecture of a Pseudomonas fluorescens biofilm", *Biotechnology and Bioengineering*, **78**(2): p. 164-171.

8. Towler, B.W., C.J. Rupp, A.B. Cunningham, and P. Stoodley, (2003), "Viscoelastic Properties of a Mixed Culture Biofilm from Rheometer Creep Analysis", *Biofouling*, **19**(5): p. 279-285.

9. Throne-Holst, M., A. Wentzel, T.E. Ellingsen, H.-K. Kotlar, and S.B. Zotchev, (2007), "Identification of Novel Genes Involved in Long-Chain n-Alkane Degradation by Acinetobacter sp. Strain DSM 17874", *Appl. Environ. Microbiol.*, **73**(10): p. 3327-3332.

10. Malic, S., K.E. Hill, A. Hayes, S.L. Percival, D.W. Thomas, and D.W. Williams, (2009), "Detection and identification of specific bacteria in wound biofilms using peptide nucleic acid fluorescent in situ hybridization (PNA FISH)", *Microbiology*, **155**(8): p. 2603-2611.

11. Wagner, M., R. Erhart, W. Manz, R. Amann, H. Lemmer, D. Wedi, and K.H. Schleifer, (1994), "Development of an rRNA-targeted oligonucleotide probe specific for the genus Acinetobacter and its application for in situ monitoring in activated sludge", *Appl. Environ. Microbiol.*, **60**(3): p. 792-800.

12. Thurnheer, T., R. Gmür, and B. Guggenheim, (2004), "Multiplex FISH analysis of a six-species bacterial biofilm", *Journal of Microbiological Methods*, **56**(1): p. 37-47.

13. S. Lazzari, A.B., E. Magyari and F. Piccinini. "Dual Solutions for Viscous Mixed Convection Flows in a Vertical Circular Duct: a Numerical Benchmark". in *COMSOL*. 2007. Grenoble: COMSOL.

14. K. Buehler, J.W.L. "Numerical Simulations of Spherical Gap Flows". in *COMSOL*. 2008. Hannover.

15. Marteyn, B., F.B. Scorza, P.J. Sansonetti, and C. Tang, (2011), "Breathing life into pathogens: the influence of oxygen on bacterial virulence and host responses in the gastrointestinal tract", *Cellular Microbiology*, **13**(2): p. 171-176.

16. Ju, L.-K. and C.S. Ho, (1989), "Oxygen diffusion coefficient and solubility in n-hexadecane", *Biotechnology and Bioengineering*, **34**(9): p. 1221-1224.

17. Peng, C.-S. and T.-L. Chen, (1994), "Influence of n-hexadecane on penicillin fermentation with Penicillium chrysogenum: The morphological effect", *Biotechnology Techniques*, **8**(11): p. 773-778.